Molecular Plant Pathology

MOLECULAR PLANT PATHOLOGY (2017) 18(2), 195–209 DOI: 10.1111/mpp.12390

Broad taxonomic characterization of Verticillium wilt resistance genes reveals an ancient origin of the tomato Ve1 immune receptor

YIN SONG[1], ZHAO ZHANG[1], MICHAEL F. SEIDL[1], ALJAZ MAJER[2], JERNEJ JAKSE[2], BRANKA JAVORNIK[2] AND BART P. H. J. THOMMA[1,*]

[1]*Laboratory of Phytopathology, Wageningen University, Droevendaalsesteeg 1, 6708 PB Wageningen, the Netherlands*

[2]*Biotechnical Faculty, Agronomy Department, Centre for Plant Biotechnology and Breeding, University of Ljubljana, Jamnikarieva 101, 1000 Ljubljana, Slovenia*

SUMMARY

Plant-pathogenic microbes secrete effector molecules to establish themselves on their hosts, whereas plants use immune receptors to try and intercept such effectors in order to prevent pathogen colonization. The tomato cell surface-localized receptor Ve1 confers race-specific resistance against race 1 strains of the soil-borne vascular wilt fungus *Verticillium dahliae* which secrete the Ave1 effector. Here, we describe the cloning and characterization of *Ve1* homologues from tobacco (*Nicotiana glutinosa*), potato (*Solanum tuberosum*), wild eggplant (*Solanum torvum*) and hop (*Humulus lupulus*), and demonstrate that particular Ve1 homologues govern resistance against *V. dahliae* race 1 strains through the recognition of the Ave1 effector. Phylogenetic analysis shows that Ve1 homologues are widely distributed in land plants. Thus, our study suggests an ancient origin of the Ve1 immune receptor in the plant kingdom.

Keywords: Ave1 effector, leucine-rich repeat, receptor-like protein, RLP, *Verticillium dahliae*.

INTRODUCTION

In order to activate immune responses to ward off invading microorganisms, plants employ immune receptors that detect pathogen(-induced) ligands of various nature (Boller and Felix, 2009; Thomma *et al.*, 2011). The recognition of such ligands by immune receptors results in the activation of defence responses, which are often accompanied by a hypersensitive response (HR), in which the necrosis of plant tissue surrounding the site of attempted penetration is activated to restrict further pathogen invasion.

Verticillium wilts are vascular wilt diseases caused by soil-borne fungal pathogens that belong to the *Verticillium* genus. *Verticillium dahliae* is the most notorious species and can infect hundreds of dicotyledonous hosts (Fradin and Thomma, 2006; Inderbitzin *et al.*, 2011). In tomato (*Solanum lycopersicum*), the *Ve* locus that confers race-specific resistance against *Verticillium* has been characterized (Fradin *et al.*, 2009; Kawchuk *et al.*, 2001). This locus contains two closely linked and inversely oriented genes, *Ve1* and *Ve2*, which encode extracellular leucine-rich repeat receptor-like proteins (eLRR-RLPs) (Kawchuk *et al.*, 2001; Wang G *et al.*, 2008, 2010). Of these, only *Ve1* was found to provide *V. dahliae* resistance in tomato (Fradin *et al.*, 2009). Interestingly, interfamily transfer of *Ve1* from tomato to Arabidopsis resulted in *Verticillium* resistance in the latter species (Fradin *et al.*, 2011, 2014; Zhang *et al.*, 2014), implying that the underlying immune signalling pathway is conserved (Fradin *et al.*, 2011; Thomma *et al.*, 2011).

Comparative genomics of *V. dahliae* race 1 and 2 strains identified the Ave1 effector that activates Ve1-mediated immunity (de Jonge *et al.*, 2012). Interestingly, *Ave1* homologues were found in the bacterial plant pathogen *Xanthomonas axonopodis* pv. *citri* (*XacPNP*) and in the plant-pathogenic fungi *Colletotrichum higginsianum* (*ChAve1*), *Cercospora beticola* (*CbAve1*) and *Fusarium oxysporum* f. sp. *lycopersici* (*FoAve1*), and these homologues were differentially recognized by Ve1 (de Jonge *et al.*, 2012). During the optimization of an agroinfiltration assay in tobacco for the functional analysis of Ve1 signalling, we found that the expression of *Ave1* in leaves of *Nicotiana glutinosa* triggered an HR, suggesting that this species contains an endogenous *Ve1* allele (Zhang *et al.*, 2013a). Indeed, inoculation experiments revealed that *N. glutinosa* is resistant to race 1 *V. dahliae*, whereas an *Ave1* deletion strain was able to cause *Verticillium* wilt disease on these plants (Zhang *et al.*, 2013a).

So far, several *Ve1* homologues have been identified within and outside the Solanaceae family, such as *SlVe1* from *Solanum lycopersicoides* (Chai *et al.*, 2003), *StVe1* from *S. tuberosum* (Simko *et al.*, 2004a), *StVe* and *StoVe1* from *S. torvum* (Fei *et al.*, 2004; Liu *et al.*, 2012), *mVe1* from *Mentha longifolia* (Vining and Davis, 2009), *Vr1* from *Lactuca sativa* (Hayes *et al.*, 2011), *VvVe* from *Vitis vinifera* (Tang *et al.*, 2016) and *GbVe*, *Gbve1*, *Gbvdr5* and *Gbvdr3* from *Gossypium barbadense* (Chen *et al.*, 2016; Yang *et al.*, 2014; Zhang *et al.*, 2011, 2012). However, the functionality of these homologues against *Verticillium* wilt often remains obscure. Here, we describe the cloning and functional

* *Correspondence*: Email: bart.thomma@wur.nl

characterization of *Verticillium* wilt resistance genes from tobacco (*N. glutinosa*), potato (*S. tuberosum*), wild eggplant (*S. torvum*) and hop (*Humulus lupulus*), and demonstrate that particular Ve1 homologues govern resistance against *V. dahliae* race 1 strains through the recognition of the Ave1 effector.

RESULTS

Isolation of *NgVe1* from *N. glutinosa*

In our first attempt to clone the previously identified *Ve1* homologue from *N. glutinosa* (Zhang *et al.*, 2013a), a single cDNA fragment of ~2800 bp was obtained using primers that were designed on the tomato *Ve1* sequence (Table S1, see Supporting Information). To obtain the full-length *N. glutinosa Ve1* (*NgVe1*) transcript sequence, 3′ rapid amplification of cDNA ends (RACE) polymerase chain reaction (PCR) was performed, resulting in a single fragment of approximately 1200 bp. Likewise, a fragment of approximately 640 bp was amplified with 5′ RACE (Methods S1, see Supporting Information). The sequences of the three fragments were aligned to deduce the full-length *NgVe1* cDNA sequence. Subsequently, a pair of *NgVe1*-specific primers (NgVe1-F and NgVe1-R; Table S1) was designed and amplicons amplified from *N. glutinosa* cDNA and genomic DNA were sequenced, indicating that both amplicons are identical (GenBank accession: KT895339) and that *NgVe1* is an intronless gene.

The full-length cDNA of *NgVe1* is 3225 bp and contains a predicted translation initiation site (ATG) at nucleotide position 34 and a stop codon (TGA) at nucleotide position 3178, resulting in a single open reading frame of 3147 bp. The predicted NgVe1 protein comprises 1048 amino acids (GenBank accession: ALK26499) and shares an overall identity of 76% with tomato Ve1 (Fig. S1, see Supporting Information). Immunoblotting analysis using green fluorescent protein (GFP) antibody displayed clear signals for NgVe1-GFP and Ve1-GFP in transiently transformed tobacco leaves (Fig. S2, see Supporting Information).

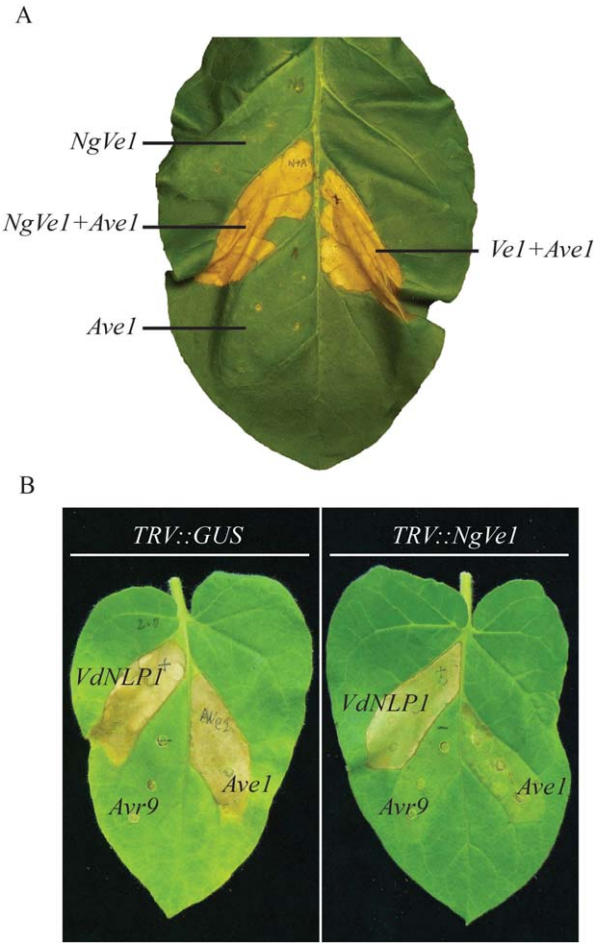

Fig. 1 Expression of *NgVe1* in tobacco mediates the Ave1-triggered hypersensitive response (HR). (A) Co-expression of *NgVe1* and *Ave1* in tobacco results in an HR. Photographs were taken at 5 days post-infiltration and show representative leaves of at least three independent assays. As a positive control, HR was induced on co-infiltration of *Ve1* and *Ave1*. As a negative control, *NgVe1* and *Ave1* were expressed separately. (B) Ave1-triggered HR, but not VdNLP1-mediated cell death, is attenuated in *NgVe1*-silenced *Nicotiana glutinosa* plants, whereas Avr9 does not trigger cell death.

Co-expression of *Ave1* and *NgVe1* induces an HR in *N. tabacum*

Recently, an optimized agroinfiltration assay has been developed for Ve1-mediated immune signalling in *N. tabacum*, revealing a swift HR on co-expression of tomato *Ve1* with *V. dahliae Ave1* (Zhang *et al.*, 2013a). To test the functionality of *NgVe1*, co-expression with *Ave1* on agroinfiltration in *N. tabacum* was performed. At 5 days post-infiltration, the infiltrated leaves developed clear necrosis, and the HR induced on co-expression of *NgVe1* and *Ave1* was as strong as the HR induced on co-infiltration of tomato *Ve1* and *Ave1*, for which the complete infiltrated areas became fully necrotic (Fig. 1A). In contrast, agroinfiltration of *NgVe1* or *Ave1* alone did not induce necrosis (Fig. 1A). These data strongly suggest that *NgVe1* is a functional homologue of tomato *Ve1*.

Targeting of *NgVe1* expression in *N. glutinosa* compromises Ave1-induced HR, but not *Verticillium* resistance

To investigate the role of *NgVe1* in *N. glutinosa Verticillium* resistance, we used virus-induced gene silencing (VIGS). *Tobacco rattle virus* (TRV)-based VIGS is a well-established method for gene functional analysis in several Solanaceae species, and also for the investigation of Ve1-mediated *Verticillium* resistance (Fradin *et al.*, 2009; Senthil-Kumar *et al.*, 2007; Zhang *et al.*, 2013a). In an attempt to establish VIGS in *N. glutinosa*, a 1 : 1 mixture of

Agrobacterium tumefaciens cultures carrying *pTRV1* and *pTRV2::PDS* to target the *phytoene desaturase* (*PDS*) gene was infiltrated into cotyledons of *N. glutinosa* plants. Visible photobleaching symptoms were observed in all agroinfiltrated *N. glutinosa* plants by 4 weeks post-infiltration (Fig. S3A, see Supporting Information), albeit that a strongly varying degree of photobleaching was observed (Fig. S3A). Nevertheless, a recombinant TRV vector was designed to target *NgVe1* expression (*pTRV2::NgVe1*). As a negative control, a construct (*pTRV2::GUS*) containing a fragment of the *β-glucuronidase* (*GUS*) gene was used. At 4 weeks after TRV infection, mature leaves were agroinfiltrated to express *Ave1*, with *VdNLP1* as a positive control (Santhanam *et al.*, 2013) and the functionally and structurally unrelated effector *Avr9* from the tomato leaf mould pathogen *Cladosporium fulvum* as a negative control (van Kan *et al.*, 1991; Van der Hoorn *et al.*, 2000). Agroinfiltration of *Ave1* in *N. glutinosa* on *GUS* targeting resulted in a clear HR within 5 days, confirming that TRV infection did not compromise Ve1-mediated HR (Fig. 1B). However, targeting of *NgVe1* expression in *N. glutinosa* significantly compromised HR on expression of *Ave1* (Fig. 1B). As expected, VdNLP1-mediated cell death was not compromised on targeting of *NgVe1* expression, whereas Avr9 expression never triggered HR (Fig. 1B).

To test the role of *NgVe1* in *Verticillium* resistance, 3 weeks after TRV inoculation, plants were challenged with either *V. dahliae* race 1 strain JR2 (Faino *et al.*, 2015) or a transformant from which the *Ave1* gene had been deleted (*V. dahliae* JR2Δ*Ave1*; de Jonge *et al.*, 2012), and monitored for disease development (stunting, wilting, chlorosis and necrosis) up to 14 days post-inoculation (dpi). As expected, no disease symptoms were observed in *N. glutinosa* plants on *GUS* targeting and subsequent mock inoculation or on inoculation with *V. dahliae* JR2, whereas the *Ave1* deletion strain caused clear *Verticillium* wilt disease (Fig. S3B). However, unexpectedly, in repeated assays, no *Verticillium* wilt symptoms were observed on *NgVe1* targeting and subsequent inoculation with *V. dahliae* (Fig. S3B). However, in line with the extremely variable photobleaching (Fig. S3A), assessment of the silencing efficiency revealed only a slight reduction in *NgVe1* expression in *NgVe1*-targeted *N. glutinosa* plants when compared with *GUS*-silenced plants (Fig. S3C), and attempts to increase the silencing efficiency were unsuccessful. These results confirm previous observations that *N. glutinosa* is not very amenable to TRV-based VIGS (Senthil-Kumar *et al.*, 2007; Zhang *et al.*, 2013a) and, furthermore, suggest that the moderate silencing efficiency obtained in our experiments is sufficiently high to compromise NgVe1-mediated HR, but insufficient to compromise NgVe1-mediated resistance.

Expression of *NgVe1* in Arabidopsis confers *Verticillium* resistance

As TRV-based VIGS did not appear to be very suitable for gene functional analysis in *N. glutinosa*, we pursued other strategies to functionally characterize *NgVe1*. We have shown previously that interfamily transfer of tomato *Ve1* to Arabidopsis results in resistance to race 1 *Verticillium* strains, providing a relatively fast method to assess Ve1 functionality (Fradin *et al.*, 2011, 2014; Zhang *et al.*, 2014). To further confirm functionality in *Verticillium* resistance, heterologous expression in Arabidopsis was obtained (Fig. S4, see Supporting Information). No obvious developmental alterations were observed in transgenic plants when compared with wild-type plants (Fig. 2A) and, subsequently, three independent *NgVe1*-transgenic lines (*NgVe1-1*, *NgVe1-2* and *NgVe1-3*), as well as transgenic plants expressing tomato *Ve1* (Fradin *et al.*, 2011) and non-transgenic controls, were inoculated with *V. dahliae* JR2. Interestingly, like tomato *Ve1*-expressing plants, *NgVe1*-transgenic plants were clearly resistant to race 1 *V. dahliae*, as significantly fewer *Verticillium* wilt symptoms were observed when compared with non-transgenic control plants (Fig. 2A,B). In contrast, *NgVe1* and *Ve1* transgenic plants were as diseased as non-transgenic controls on inoculation with the *Ave1* deletion strain (Fig. 2A,B). These data are further supported by fungal biomass quantifications which revealed significantly reduced fungal accumulation in *NgVe1*-transgenic and *Ve1*-expressing Arabidopsis plants for *V. dahliae* carrying *Ave1*, but not for the *Ave1* deletion mutant, when compared with wild-type Arabidopsis plants (Fig. 2C). Collectively, these data confirm that NgVe1 acts as a functional homologue of tomato Ve1 that recognizes race 1 *V. dahliae*.

Cloning and functional analysis of *Ve1* homologues from potato and wild eggplant

Ve gene homologues occur in the solanaceous species *S. lycopersicoides* (*SlVe1*; Chai *et al.*, 2003) and the wild eggplant species *S. torvum* (*StVe* and *StoVe1*; Fei *et al.*, 2004; Liu *et al.*, 2012). Moreover, in tetraploid potato (*S. tuberosum*), a quantitative trait locus (QTL) for *Verticillium* resistance was identified using the tomato *Ve1* gene as a probe. This locus was found to contain at least 11 genes, all putatively encoding LRR-type receptor-like proteins (Simko *et al.*, 2004a). The tomato and potato genomes are highly collinear and the QTL locus was mapped to a region on potato chromosome 9 that is syntenic to the short arm of tomato chromosome 9 that carries *Ve1* and *Ve2* (Diwan *et al.*, 1999; Simko *et al.*, 2004b). Subsequently, this *Verticillium* resistance QTL locus was annotated and found to contain two predicted *receptor-like protein 12-like* genes [National Center for Biotechnology Information (NCBI): XM_006362308 and XM_006362309] in the genome sequence of *S. tuberosum* group Phureja DM1-3 516 R44 (Xu *et al.*, 2011). Here, the coding sequences (CDSs) of *Ve* gene homologues were amplified from cDNA of the heterozygous diploid potato breeding line *S. tuberosum* group Tuberosum RH 89-039-16 (Xu *et al.*, 2011), sequenced and submitted to NCBI as *StuVe1* and *StuVe2* (GenBank accessions: KT946795 and

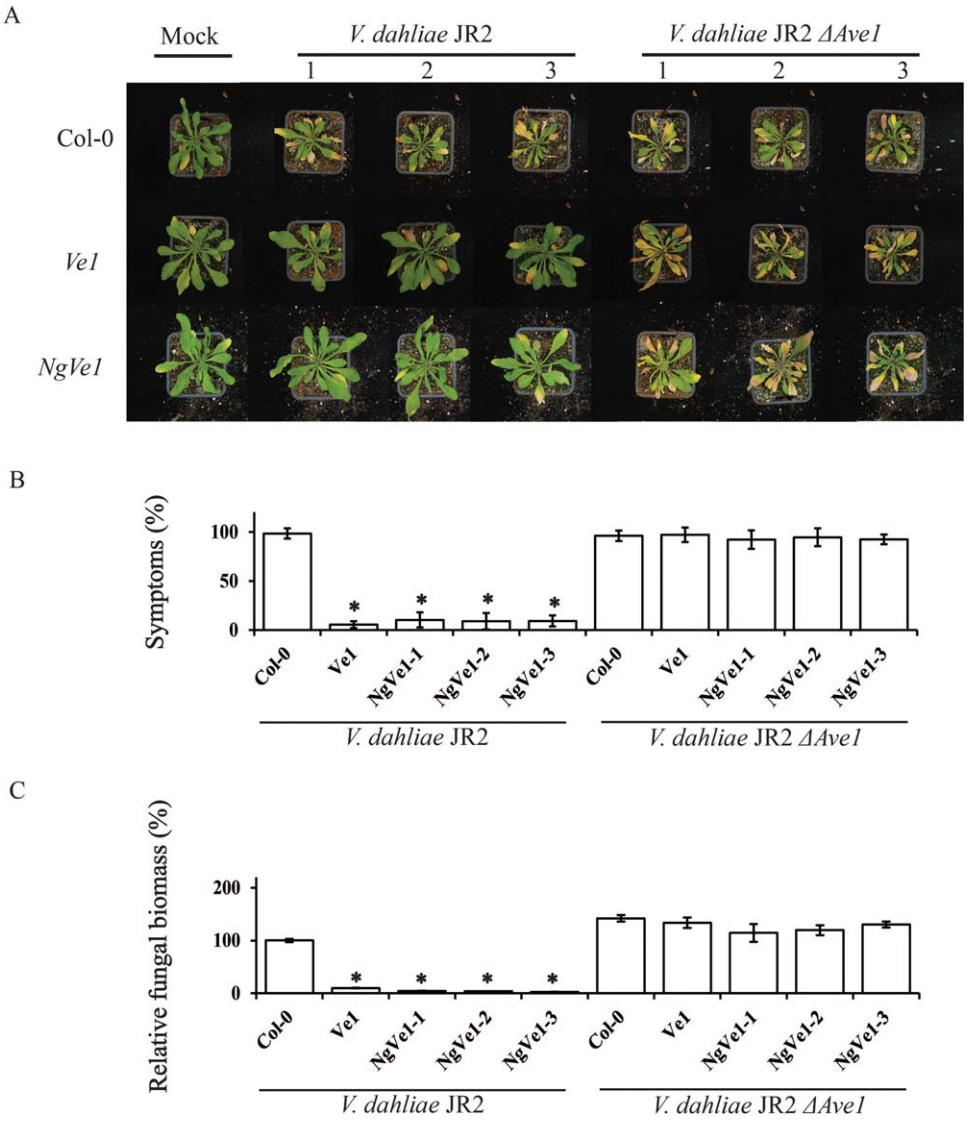

Fig. 2 Expression of *NgVe1* in Arabidopsis mediates resistance against race 1 *Verticillium dahliae*. (A) Typical appearance of non-transgenic Arabidopsis and transgenic lines that constitutively express *NgVe1* on mock inoculation or inoculation with *V. dahliae* strain JR2 or *V. dahliae* JR2 Δ*Ave1* at 21 days post-inoculation (dpi). (B) Quantification of *Verticillium* wilt symptoms in Arabidopsis Col-0 and transgenic plants at 21 dpi. Bars represent quantification of symptom development as the percentage of diseased rosette leaves with standard deviation, with Col-0 (control) set to 100%. (C) Fungal biomass determined by quantitative real-time polymerase chain reaction in Arabidopsis Col-0 and transgenic plants at 21 dpi. Bars represent *Verticillium* internal transcribed spacer (ITS) transcript levels relative to AtRuBisCo (RuBisCo, ribulose-1,5-bisphosphate carboxylase/oxygenase) transcript levels (for equilibration) with standard deviation in a sample of five pooled plants. The fungal biomass in Col-0 (control) is set to 100%. Three independent lines are shown (1, 2 and 3). Asterisks indicate significant differences when compared with Col-0 ($P < 0.05$). *Ve1* transgenic plants were used as a positive control. The data shown are representative of at least three independent experiments.

KT946797) (Methods S1). The predicted StuVe1 and StuVe2 proteins are composed of 1053 and 1138 amino acids (GenBank accessions: ALK26501 and ALK26503), respectively, and share 87% and 84% identity with tomato Ve1 and 81% and 91% identity with tomato Ve2, respectively, and 82% identity with each other (Fig. S1).

To study the composition of the *Ve* locus in wild eggplant, the CDSs of *Ve* gene homologues were cloned from the cDNA of the *Verticillium*-resistant *S. torvum* genotype Tuolubamu, sequenced and deposited at NCBI as *StoVe1* and *StoVe2* (GenBank accessions: KT946794 and KT946796) (Methods S1). The predicted StoVe1 and StoVe2 proteins comprise 1051 and 1135 amino acids (GenBank accessions: ALK26500 and ALK26502), respectively, and share 83% and 80% identity with tomato Ve1 and 81% and 85% identity with tomato Ve2, respectively, and 92% identity with each other (Fig. S1).

To check the functionality of *StuVe1*, *StuVe2*, *StoVe1* and *StoVe2*, mature tobacco leaves were co-infiltrated with a 1 : 1 mixture of *A. tumefaciens* cultures carrying *Ave1* and the various *Ve1* homologues. Intriguingly, agroinfiltration in at least three independent assays revealed that the expression of *Ave1* together with *StuVe1* or *StoVe1* induced signs of a weak HR at 5 days post-infiltration (Fig. 3A). However, when compared with the HR induced on co-agroinfiltration of tomato *Ve1* and *Ave1*, only a minor part of the infiltrated region developed necrosis (Fig. 3A). Agroinfiltration of *Ave1* with *StuVe2* or *StoVe2* induced no such responses at all (Fig. 3A). Immunoblotting confirmed that the StuVe1, StuVe2, StoVe1 and StoVe2 fusion proteins were expressed (Fig. 3B).

As VIGS-based gene silencing in potato genotype Tuberosum RH 89-039-16 and wild eggplant genotype Tuolubamu has not been established, we did not attempt VIGS-based assays to test the role of these *Ve1* homologues in *Verticillium* resistance. Rather,

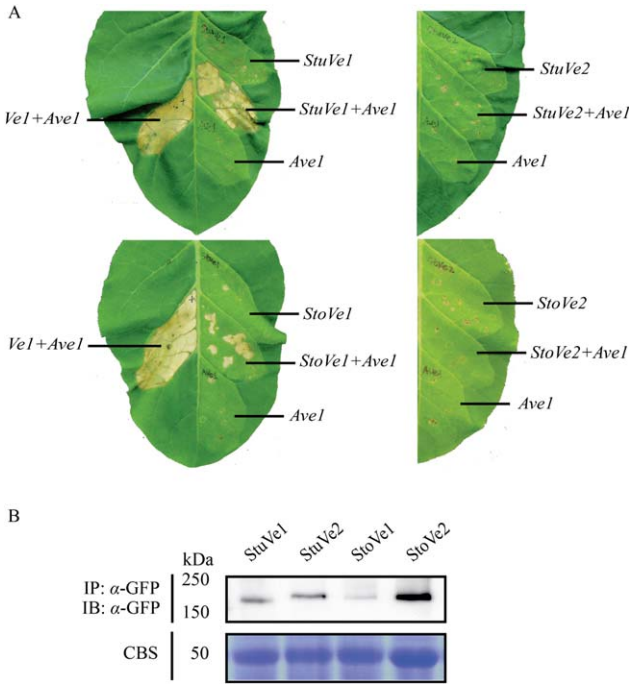

Fig. 3 StuVe1 and StoVe1, but not StuVe2 and StoVe2, recognize Ave1 in *Nicotiana tabacum*. (A) Co-expression of *StuVe1* and *StoVe1*, but not *StuVe2* and *StoVe2*, with *Ave1* in tobacco induces signs of a relatively weak hypersensitive response (HR). Photographs were taken at 5 days post-infiltration and show representative leaves of at least three independent assays. As a positive control, HR was induced on co-infiltration of *Ve1* and *Ave1*. As a negative control, *StuVe1*, *StuVe2*, *StoVe1*, *StoVe2* and *Ave1* were expressed separately. (B) Green fluorescent protein (GFP)-tagged StuVe1, StuVe2, StoVe1 and StoVe2 proteins are detected in planta by immunopurification (IP) using GFP-affinity beads, followed by immunoblotting (IB) using α-GFP antibody. Coomassie blue staining (CBS) of the blot containing total protein extracts showed equal loading in each lane based on the 50-kDa RuBisCo (ribulose-1,5-bisphosphate carboxylase/oxygenase) band.

heterologous expression in Arabidopsis was pursued (Fig. S4). No developmental alterations were observed in transgenic plants when compared with *Ve1*-expressing and wild-type plants (Fig. 4A), and three independent transgenic lines expressing *StuVe1*, *StuVe2*, *StoVe1* or *StoVe2* were assayed for *V. dahliae* resistance. Intriguingly, despite the weak HR observed on agroinfiltration together with *Ave1* in *N. tabacum*, *StoVe1*- and *StuVe1*-expressing plants were clearly resistant to race 1 *V. dahliae* strain JR2, similar to *Ve1*-transgenic plants (Fig. 4A,B). In contrast, *StuVe2* and *StoVe2* transgenes were as diseased as non-transgenic controls (Fig. 4A,B). Importantly, all genotypes were equally susceptible to the *V. dahliae Ave1* deletion mutant (Fig. 4A,B), suggesting that all of these *Ve1* alleles recognize the Ave1 effector. The phenotypes correlated with the degree of *V. dahliae* colonization as determined by real-time PCR (Fig. 4). Collectively, these data confirm that StuVe1 and StoVe1, but not StuVe2 and StoVe2, act as functional homologues of tomato Ve1 that confer resistance to race 1 *V. dahliae*.

HLVe1-2A, but not HLVe1-2B, recognizes *Verticillium* effector Ave1

Polygenic resistance to *Verticillium* spp. has also been described in several non-solanaceous species, including hop, alfalfa, cotton and strawberry (Antanaviciute *et al.*, 2015; Bolek *et al.*, 2005; Jakse *et al.*, 2013; Wang HM *et al.*, 2008; Yang *et al.*, 2008). Genetic resistance against *Verticillium* wilt in hop (*Humulus lupulus*) was introduced into breeding programmes from American wild hop (*H. lupulus* var. *neomexicanus*) and is still used today as the main resistance source (Darby, 2001). Genetic analysis identified a single significant QTL for this resistance, suggesting that *Verticillium* wilt resistance in hop is conferred by more than a single gene (Jakse *et al.*, 2013; Majer *et al.*, 2014). To investigate the presence of *Ve*-like sequences in hop, Southern blotting with the tomato *Ve1* gene as probe was performed, revealing low copy numbers of *Ve*-like sequences in hop cultivars (Fig. S5 and Methods S1, see Supporting Information). With thermal asymmetric interlaced (TAIL)-PCR (Terauchi and Kahl, 2000), several *Ve*-like sequences were identified (Methods S1). Further analysis revealed two *Ve1* alleles in the *Verticillium*-resistant hop cultivar 'Wye Target', designated *HLVe1-2A* (GenBank accession: KJ647426) and *HLVe1-2B* (GenBank accession: KJ647427), which both encode 1039-amino-acid proteins (GenBank accessions: AIE39594 and AIE39595) sharing 52% and 51% identity with tomato *Ve1* and *Ve2*, respectively, and 98% identity with each other (Fig. S1). To investigate the functionality of *HLVe1-2A* and *HLVe1-2B* in *Verticillium* resistance, co-agroinfiltration with *Ave1* in *N. tabacum* was performed. When mature tobacco leaves were co-infiltrated

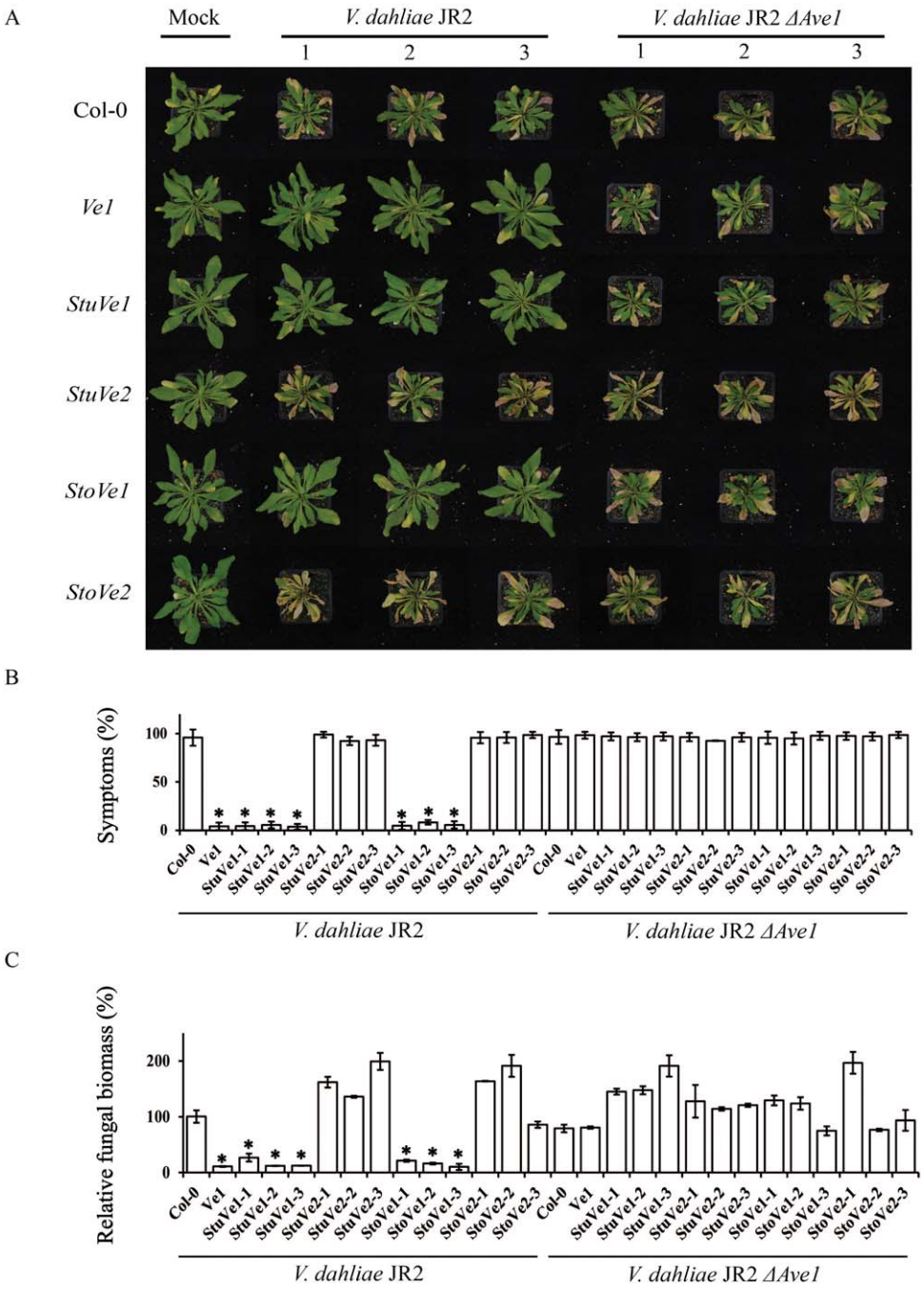

Fig. 4 StuVe1 and StoVe1, but not StuVe2 and StoVe2, provide resistance against race 1 *Verticillium dahliae* in Arabidopsis. (A) Typical appearance of non-transgenic Arabidopsis and transgenic plants that were engineered to express 35S-driven *StuVe1*, *StuVe2*, *StoVe1* or *StoVe2* on mock inoculation or inoculation with *V. dahliae* JR2 or *V. dahliae* JR2 Δ*Ave1* at 21 days post-inoculation (dpi). (B) Quantification of *Verticillium* wilt symptoms in Arabidopsis Col-0 and transgenic plants at 21 dpi. Bars represent the quantification of symptom development as the percentage of diseased rosette leaves with standard deviation, with Col-0 (control) set to 100%. (C) Fungal biomass determined by quantitative real-time polymerase chain reaction in Arabidopsis Col-0 and transgenic plants at 21 dpi. Bars represent *Verticillium* internal transcribed spacer (ITS) transcript levels relative to AtRuBisCo (RuBisCo, ribulose-1,5-bisphosphate carboxylase/oxygenase) transcript levels (for equilibration) with standard deviation in a sample of five pooled plants. The fungal biomass in Col-0 (control) is set to 100%. Three independent lines are shown (1, 2 and 3). Asterisks indicate significant differences when compared with Col-0 ($P < 0.05$). *Ve1* transgenic plants were used as a positive control. The data shown are representative of at least three independent experiments.

with a 1 : 1 mixture of *A. tumefaciens* cultures carrying *Ave1* and *HLVe1-2A*, signs of a weak HR were observed at 5 days post-infiltration with a minor part of the infiltrated region developing necrosis (Fig. 5A). However, in contrast, co-expression of *Ave1* and *HLVe1-2B* in tobacco induced no such response, similar to the co-agroinfiltration of *Ve1*, *HLVe1-2A* and *HLVe1-2B* with *Avr9* (Fig. 5A). To test whether the failure of HLVe1-2B to induce an HR was the result of the instability of the protein, the coding regions of *HLVe1-2A* and *HLVe1-2B* were cloned to generate C-terminally GFP-tagged expression constructs, and the stability of both proteins was verified by immunoblotting (Fig. 5B).

To further assess the role of *HLVe1-2A* and *HLVe1-2B* in resistance to *V. dahliae*, heterologous expression in Arabidopsis was pursued (Fig. S4). No phenotypic alterations were observed in plants that expressed *HLVe1-2A* or *HLVe1-2B* when compared with *Ve1*-transgenic or non-transgenic plants (Fig. 6A), and three independent transgenic lines for *HLVe1-2A* and *HLVe1-2B* were assayed for *V. dahliae* resistance. Interestingly, despite the weak

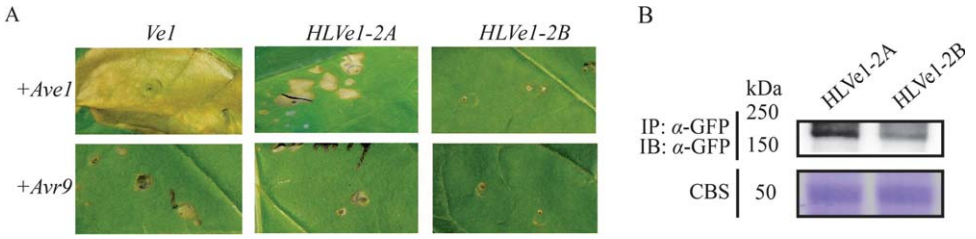

Fig. 5 Co-expression of *HLVe1-2A*, but not *HLVe1-2B*, with *Ave1* in *Nicotiana tabacum* activates a hypersensitive response (HR). (A) *HLVe1-2A* or *HLVe1-2B* was transiently co-expressed with *Ave1* in *N. tabacum*. As a negative control, *Avr9* was co-expressed with *Ve1* homologues. As a positive control, HR was induced on co-expression of *Ve1* and *Ave1*. (B) Green fluorescent protein (GFP)-tagged HLVe1-2A and HLVe1-2B proteins are detected in planta by immunopurification (IP) using GFP-affinity beads, followed by immunoblotting (IB) using α-GFP antibody. Coomassie blue staining (CBS) of the blot containing total protein extracts showed equal loading in each lane based on the 50-kDa RuBisCo (ribulose-1,5-bisphosphate carboxylase/oxygenase) band.

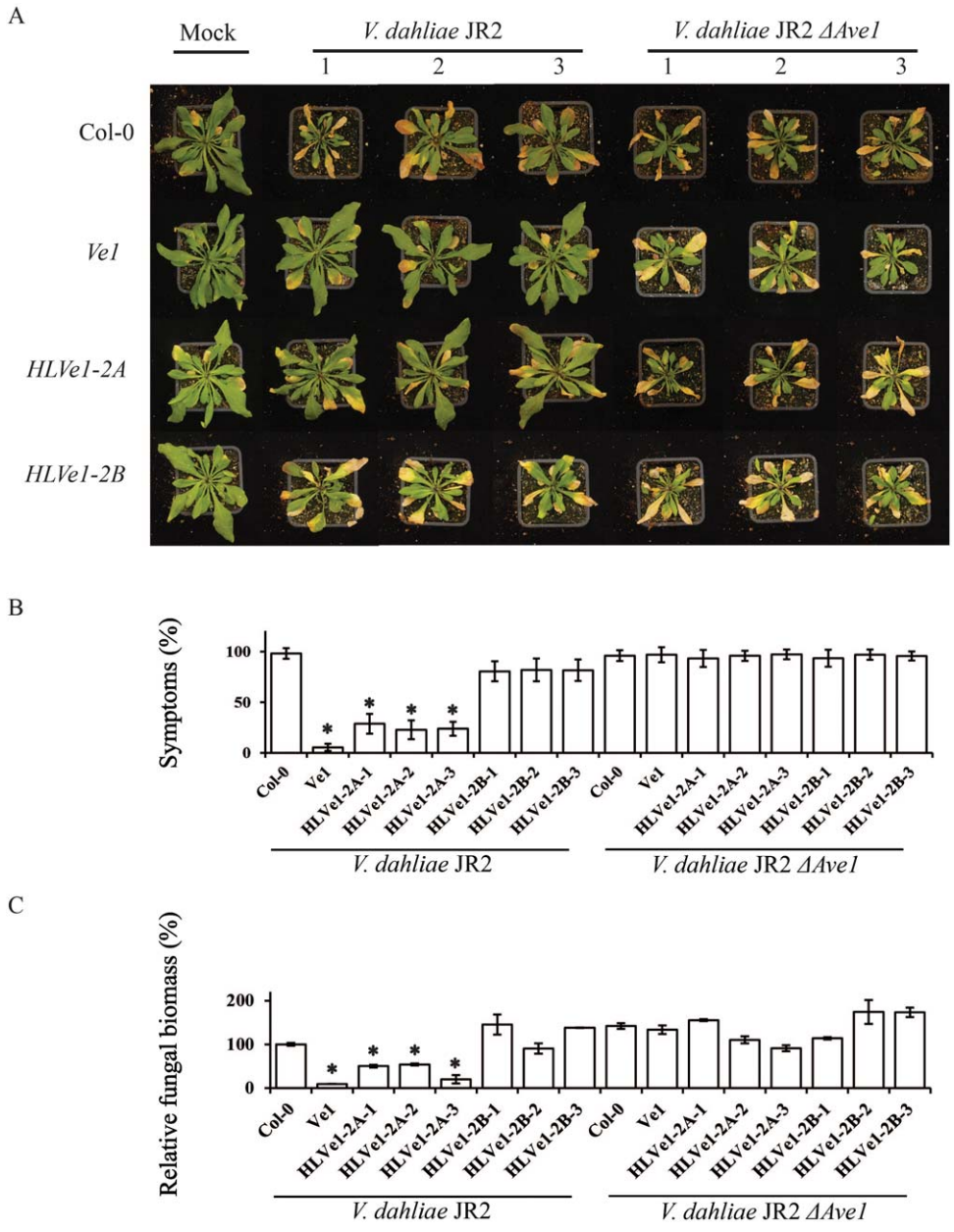

Fig. 6 *HLVe1-2A*, but not *HLVe1-2B*, confers resistance to race 1 *Verticillium dahliae* in Arabidopsis. (A) Typical appearance of non-transgenic Arabidopsis and transgenic lines that constitutively express *HLVe1-2A* or *HLVe1-2B* on mock inoculation or inoculation with *V. dahliae* strain JR2 or *V. dahliae* JR2 Δ*Ave1* at 21 days post-inoculation (dpi). (B) Quantification of *Verticillium* wilt symptoms in Arabidopsis Col-0 and transgenic lines at 21 dpi. Bars represent the quantification of symptom development as the percentage of diseased rosette leaves with standard deviation, with Col-0 (control) set to 100%. (C) Fungal biomass determined by quantitative real-time polymerase chain reaction in Arabidopsis Col-0 and transgenic plants at 21 dpi. Bars represent *Verticillium* internal transcribed spacer (ITS) transcript levels relative to AtRuBisCo (RuBisCo, ribulose-1,5-bisphosphate carboxylase/oxygenase) transcript levels (for equilibration) with standard deviation in a sample of five pooled plants. The fungal biomass in Col-0 (control) is set to 100%. Three independent lines are shown (1, 2 and 3). Asterisks indicate significant differences when compared with Col-0 ($P < 0.05$). *Ve1* transgenic plants were used as a positive control. The data shown are representative of at least three independent experiments.

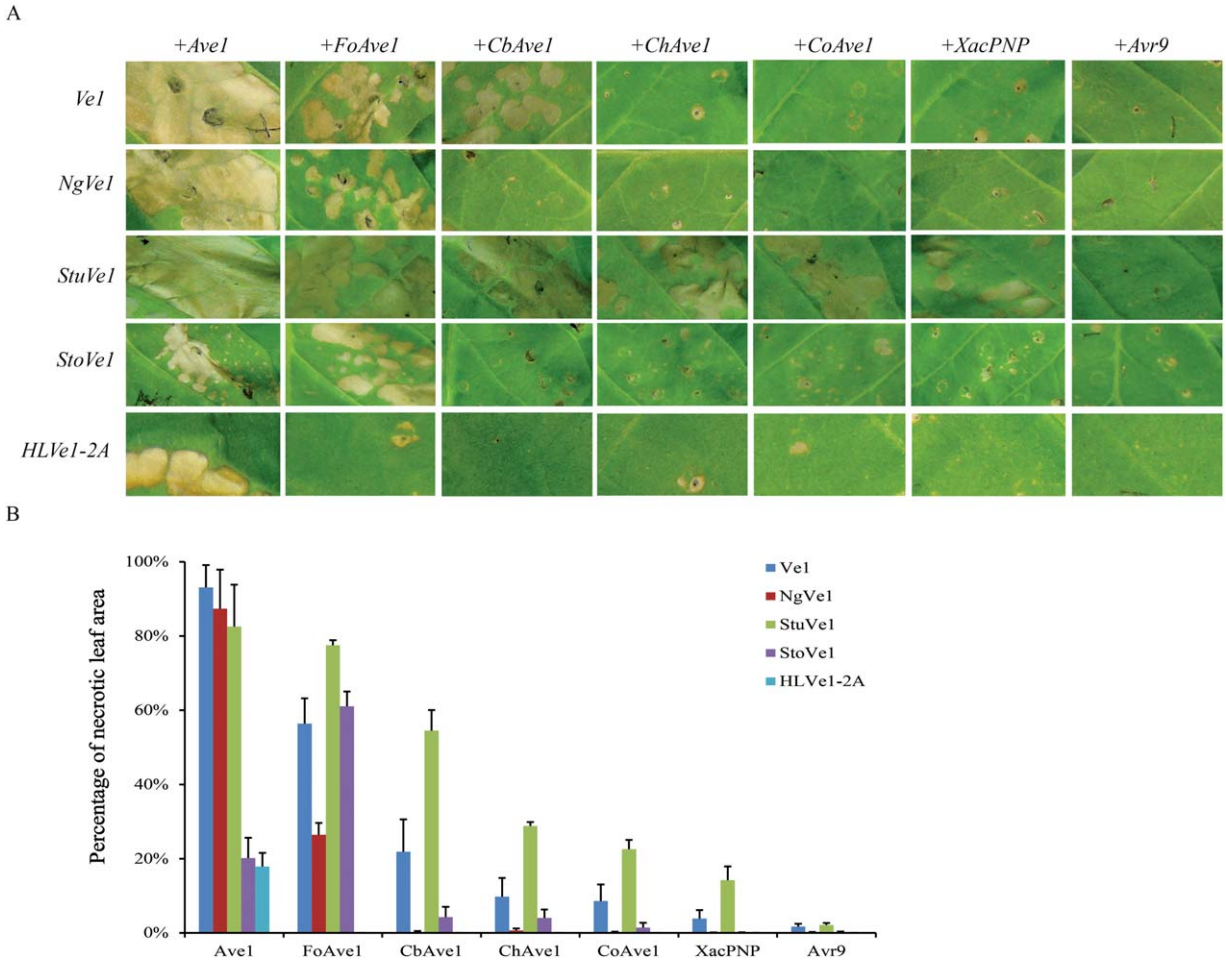

Fig. 7 Distinct necrosis induced by *Ave1* homologues through co-expression with functional *Ve1* orthologues in *Nicotiana tabacum*. (A) Co-expression of functional *Ve1* orthologues with *Ave1* homologues (*Ave1*, *FoAve1*, *CbAve1*, *ChAve1*, *CoAve1* and *XacPNP*) in *N. tabacum*. Expression of *Avr9* in combination with *Ve1* homologues is shown as a negative control. Leaves were photographed at 5 days post-infiltration to visualize necrosis resulting from recognition by functional Ve1 homologues. (B) Quantification of necrosis resulting from the recognition of Ave1 homologues by functional Ve1 orthologues at 5 days post-infiltration. Bars represent the average percentage of necrotic leaf area of infiltration zones with standard deviation.

HR observed on agroinfiltration together with *Ave1* in *N. tabacum*, *HLVe1-2A*-expressing plants were clearly resistant to *V. dahliae* race 1 strain JR2 as few, if any, symptoms were observed (Fig. 6A,B). In contrast, *HLVe1-2B* transgenic plants were as susceptible as non-transgenic controls (Fig. 6A,B), and all genotypes were equally susceptible to the *V. dahliae Ave1* deletion mutant (Fig. 6A,B). The phenotypes correlated with the level of *V. dahliae* biomass as determined by real-time PCR (Fig. 6). Collectively, these data verify that HLVe1-2A, but not HLVe1-2B, acts a functional Ve1 homologue that provides resistance to race 1 *V. dahliae*.

Functional Ve1 homologues mediate the recognition of Ave1 homologues from multiple plant pathogens

We have shown previously that tomato Ve1 recognizes not only *V. dahliae* and *V. albo-atrum* Ave1, but also homologues derived from *F. oxysporum* f. sp. *lycopersici* (FoAve1) and *C. beticola* (CbAve1) (de Jonge *et al.*, 2012). To investigate whether the newly identified functional Ve1 homologues similarly recognize these Ave1 homologues, co-expression of the five functional *Ve1* homologues with a series of *Ave1* homologues [*FoAve1*, *CbAve1*, *ChAve1*, *CoAve1* (*Colletotrichum orbiculare*; Gan *et al*, 2013) and *XacPNP* (Gottig *et al.*, 2008)] was performed (Fig. 7A). Co-expression of the effector *Avr9* (van Kan *et al.*, 1991; Van der Hoorn *et al.*, 2000) in combination with the *Ve1* homologues was used as a negative control. To compare the HR induced on co-expression of *Ave1* homologues and functional *Ve1* homologues in tobacco, HR development was measured by quantification of the leaf area that developed necrosis at 5 days post-infiltration (Fig. 7B). Co-expression of *Ve1* with *FoAve1* and *CbAve1*, but not with *ChAve1*, *CoAve1* and *XacPNP*, in *N. tabacum* resulted in HR (Fig. 7). StuVe1 seems to recognize a wider panel of Ave1

homologues, as co-expression with *Ave1*, *FoAve1*, *CbAve1*, *ChAve1*, *CoAve1* and *XacPNP* induced HR (Fig. 7). For *NgVe1* and *StoVe1*, co-infiltration with *Ave1* and *FoAve1* induced HR, whereas infiltration with *CbAve1*, *ChAve1*, *CoAve1* and *XacPNP* failed to induce HR (Fig. 7). Finally, the most narrow recognition spectrum is observed for HLVe1-2A which recognizes none of the Ave1 homologues apart from that from *V. dahliae* (Fig. 7). These data demonstrate that the newly identified functional Ve1 homologues, similar to tomato Ve1, differentially recognize Ave1 homologues from different plant pathogens.

Comparison of the protein sequences of Ve1 homologues

Tomato Ve1 is predicted to contain a signal peptide, an eLRR domain composed of two eLRR regions, separated by a non-LRR island domain (also referred to as C1, C3 and C2, respectively; Figs S6 and S7, see Supporting Information), a transmembrane domain and a short cytoplasmic tail that lacks obvious motifs for intracellular signalling (Kawchuk *et al.*, 2001; Wang *et al.*, 2010; Zhang and Thomma, 2013). Alignment of the functional Ve1 protein sequences identified in this study clearly shows the typical eLRR-RLP domain architecture (Fig. S6). All Ve1 homologues contain 37 eLRR repeats in two eLRR regions that are interrupted by a non-LRR island domain (Fig. S6). Previously, we have determined that three eLRR regions are crucial for Ve1 functionality: eLRR_1 to eLRR_8, eLRR_20 to eLRR_23 and eLRR_32 to eLRR_37 (Zhang *et al.*, 2014). A comparison of the functional Ve1 homologues studied here shows that the eLRR_1 to eLRR_8 (44.2% identity) and eLRR_20 to eLRR_23 (46.5% identity) regions of the C1 domain are only slightly more conserved than the eLRR_9 to eLRR_19 (40.2% identity) and eLRR_24 to eLRR_31 (45.0% identity) regions of the C1 domain (Figs S6 and S7). A similar comparison of the C1 domains among the non-functional Ve1 homologues studied here shows that the eLRR_1 to eLRR_8 (50.2% identity) region of the C1 domain is slightly more conserved than the eLRR_9 to eLRR_19 (45.5% identity) region of the C1 domain, whereas the eLRR_20 to eLRR_23 (50.0% identity) region of the C1 domain is conserved to a similar extent to the eLRR_24 to eLRR_31 (50.3% identity) region of the C1 domain (Fig. S7). Further comparison among the functional Ve1 homologues shows that the C3 domain (eLRR_32 to eLRR_37, 48.4% identity) is more conserved than the C1 domain (43.3% identity), C2 domain (8.0% identity) and C-terminal eLRR-flanking domain (9.2% identity) (Figs S6 and S7). This result is consistent with a previous comparison of tomato eLRR-RLPs, which showed that the C3 domain is more conserved than the C1 domain (Fradin *et al.*, 2014). Finally, a comparison of the non-functional Ve1 homologues studied here shows that the C1 domain (48.7% identity) and C3 domain (eLRR_32 to eLRR_37, 53.3% identity) are more conserved than the C2 domain (8.0% identity) and C-terminal eLRR-flanking domain (7.2% identity) (Fig. S7). Collectively, these findings do not point towards a particular conservation of the three LRR regions that were previously implicated in Ve1 functionality.

Phylogenetic analysis of *Ve1* homologues in the plant kingdom

To determine the phylogenetic breadth among *Ve1* homologues in plants, we systematically queried the available genomes of 41 plant species for the occurrence of *Ve1* homologues. In these genomes, we identified 1361 bona fide *Ve1* homologues, all of which occur in land plants (embryophytes) and none in green algae (Fig. 8A). To further analyse the phylogenetic relationship of tomato Ve1 and its close homologues, we used a neighbour-joining phylogeny to guide the extraction of the tomato *Ve1* clade and the relevant sister clades (Figs 8B and S8, see Supporting Information). These sequences were used to infer a refined maximum likelihood phylogeny containing 608 *Ve1* homologues that encompass monocots and dicots. This phylogeny revealed a *Ve1* orthologous group, defined at the last common ancestor of monocots and dicots, which contains all functional *Ve1* homologues that have been described so far (Figs 8B and S8). The broad phylogenetic distribution, with homologues present in all land plants, establishes that *Ve1* is an ancient immune receptor (Figs 8 and S8), and that the last common ancestor contained at least a single, but more likely several, *Ve1*-like genes. Moreover, we inferred a *Ve1* orthologous group that comprises both monocots and dicots and includes all functional *Ve1* genes, suggesting the conservation of function within this group of genes.

DISCUSSION

In this article, we describe the cloning and characterization of *Ve1* homologues within and outside the Solanaceae family, and demonstrate that Ve1 homologues of tobacco (NgVe1), potato (StuVe1), wild eggplant (StoVe1) and hop (HLVe1-2A) act as functional homologues of tomato Ve1 by providing resistance to race 1 *V. dahliae*, mediated through the recognition of the Ave1 effector, implying that functional Ve1 homologues are conserved across plant species within and outside the Solanaceae. We further show that all functional Ve1 proteins contain a conserved domain architecture with 37 eLRR repeats (Fig. S6). It has been determined previously that two regions of the C1 domain, namely eLRR_1 to eLRR_8 and eLRR_20 to eLRR-23, are required for Ve1 functionality, probably because they contribute to ligand binding (Zhang *et al.*, 2014). Here, these regions appear to be only slightly more conserved than other regions within the functional Ve1 homologues (Figs S6 and S7). In addition, the C3 domain (eLRR_32 to eLRR_37) has been shown to be critical for Ve1 functionality (Zhang *et al.*, 2014; Fig. S6), potentially through interaction with common factors required for downstream signalling

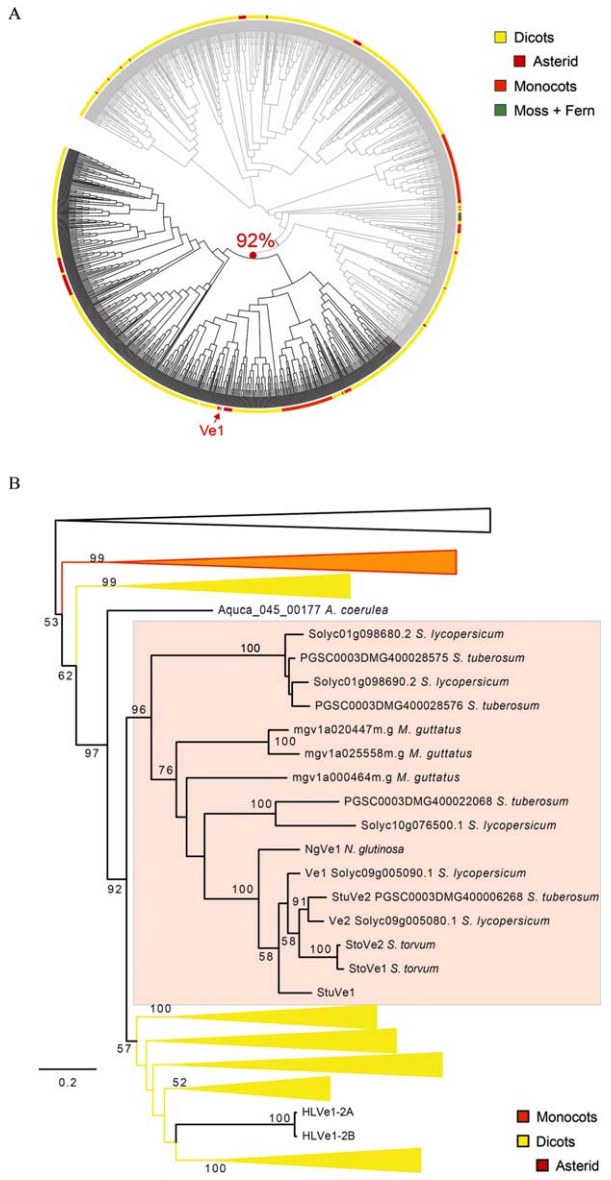

Fig. 8 Phylogenetic analysis of Ve1 homologues indicates that they are widely distributed in land plants. (A) Phylogeny of Ve1 proteins from 41 plant species from the Phytozome database. Tomato Ve1 is indicated with a red arrow. (B) Maximum likelihood phylogenetic tree of selected Ve1 homologues (dark grey clades in A) displaying the tomato Ve1 clade and the relevant sister clades. The tomato Ve1 clade is indicated by the highlighted background. Official gene identifiers and species names are indicated. Bootstrap values are shown in the tree. The scale represents the branch length expressed as the relative number of amino acid substitutions.

(Fradin *et al.*, 2014; Fritz-Laylin *et al.*, 2005; Zhang and Thomma, 2013). As expected, this region is most conserved among the functional Ve1 homologues (Figs S6 and S7). Previously, Ve1 homologues from other plant species have also been associated with *Verticillium* wilt resistance, although conclusive evidence for a causal role in resistance has mostly been lacking. For example, Vining and Davis (2009) showed that the mint *Ve1* homologue *mVe1* associates with *Verticillium* wilt resistance. Genome-wide analysis of disease resistance genes in lettuce, in combination with QTL mapping, showed that three *Ve* homologues, including *Vr1*, are located within a 100-kb region on chromosome 9 that co-segregates with resistance to race 1 *V. dahliae* (Christopoulou *et al.*, 2015; Hayes *et al.*, 2011). The grapevine *Ve1* homologue *VvVe* has been shown to enhance defence against *V. dahliae* in *N. benthamiana* (Tang *et al.*, 2016). Remarkably, cotton *Ve1* homologues *GbVe*, *Gbve1*, *Gbvdr5* and *Gbvdr3* have been shown to confer *Verticillium* resistance on ectopic expression in Arabidopsis or cotton (Chen *et al.*, 2016; Yang *et al.*, 2014; Zhang *et al.*, 2011, 2012), although this concerns *V. dahliae* isolates that do not carry the *Ave1* effector gene, and thus *Verticillium* wilt resistance cannot be mediated by Ave1 recognition in these cases (Y. Song *et al.*, unpublished data).

Previously, we have noted the absence of correlation between Ave1-induced HR and resistance through Ve1, as treatment with Ave1 leads to HR in tomato and tobacco plants that express *Ve1*, but not in *N. benthamiana* or Arabidopsis, whereas *Ve1*-transgenic Arabidopsis shows Ave1-triggered resistance (de Jonge *et al.*, 2012; Zhang *et al.*, 2013a,b). Similarly, in the present study, we observed robust resistance mediated by the *S. torvum* and hop *Ve1* homologues *StoVe1* and *HLVe1-2A*, whereas only a weak HR was observed on co-expression of Ave1. These findings suggest that the HR may occur as a consequence of Ve1/Ave1-induced immune signalling under particular conditions, but is not required for *V. dahliae* resistance (Zhang *et al.*, 2013b). This finding may also explain why we were unable to compromise *NgVe1*-mediated *V. dahliae* resistance on VIGS in *N. glutinosa*, but were able to compromise Ave1-mediated HR.

Phylogenetic analysis revealed that *Ve1* homologues are widely distributed in phylogenetically distant plant species, implying an ancient origin of the Ve1 immune receptor. Nevertheless, this origin does not imply functionality in *V. dahliae* resistance. The most obvious example is the close tomato homologue *Ve2* which, despite its homology, does not act as a functional *V. dahliae* resistance gene. Similarly, in this study, we identified the non-functional *Ve1* homologues *StuVe2*, *StoVe2* and *HLVe1-2B*. The *Ve* locus as it occurs in tomato, with two homologues *Ve1* and *Ve2*, appears to originate before speciation, as clustered *Ve1* family members also appear in potato and wild eggplant. Furthermore, a functional study addressing Ave1 recognition in the genus *Nicotiana* only identified Ave1 recognition, and thus the presence of a potentially functional *Ve1* homologue, in the species *N. glutinosa* (Zhang *et al.*, 2013a). Considering the extremely wide host range of *V. dahliae*, and the general occurrence of strains that carry *Ave1*, the question arises as to whether the ancient progenitor of the currently functional Ve1 orthologues already functioned as a *V. dahliae* resistance gene, and thus several species/

homologues lost the capacity to recognize Ave1 as a result of adverse effects associated with Ve1 functionality, or whether several species/homologues evolved the capacity to recognize Ave1 after the occurrence of speciation events. The latter hypothesis would imply that Ave1 recognition evolved multiple times in the plant kingdom through parallel evolution. Our present data do not allow the verification or disqualification of either hypothesis.

Plants and animals employ germline-encoded pattern recognition receptors (PRRs) to detect broadly distributed microbe-associated molecular patterns (MAMPs) and to activate antimicrobial defence (Macho and Zipfel, 2014). We have noted previously that tomato Ve1 is an ancient pathogen receptor with traits of typical PRRs. This finding was based on the transferability of *Ve1* across plant species and the observation that Ve1 resistance affected three fungal species: *V. dahliae*, *V. albo-atrum* and *F. oxysporum* (Fradin *et al.*, 2011; de Jonge *et al.*, 2012; Thomma *et al.*, 2011). We have now demonstrated that members of the *Ve1* gene family in *N. glutinosa*, *S. tuberosum*, *S. torvum* and *H. lupulus* encode receptors that recognize Ave1 and are able to mediate *V. dahliae* resistance in Arabidopsis. As our findings are based on stable expression in a heterologous host, we realize that definitive evidence for the role of *Ve1* homologues in disease resistance in the endogenous hosts from which the *Ve1* homologues are derived needs to be provided through targeted gene deletion in these hosts, or stable expression in susceptible genotypes of these species. We also discovered that the functional Ve1 homologues have divergent recognition specificities, suggesting that some recognize an even wider spectrum of plant pathogens than tomato Ve1 (Fig. 7). Collectively, these findings mean that Ve1 has traits of a typical race-specific resistance protein as well as of a typical PRR. Similarly, Arabidopsis RLP23 recognizes an epitope of Nep-like effector proteins (NLPs) that are widely distributed among bacteria, fungi and oomycetes (Gijzen and Nürnberger, 2006) to induce immune responses (Albert *et al.*, 2015). Thus, it is becoming apparent that MAMP receptor systems are more dynamic than generally appreciated and are conditioned in a similar manner to prototypical resistance genes (Albert *et al.*, 2015; Cook *et al.*, 2015; Shibuya and Desaki, 2015). Findings like these have inspired the proposal of the 'Invasion Model', which describes plant immunity as a surveillance system to detect invasion, in which host receptors, termed invasion pattern receptors (IPRs), detect either externally encoded or modified self-ligands that indicate invasion, termed invasion patterns (IPs) (Cook *et al.*, 2015).

EXPERIMENTAL PROCEDURES

Plant growth conditions and manipulations

Plants were grown at 21°C/19°C during 16 h/8 h light/dark photoperiods in a climate chamber or glasshouse with a relative humidity of ~75% and 100 W/m^2 supplemental light when the light intensity dropped below 150 W/m^2. Arabidopsis transformations were performed as described previously (Clough and Bent, 1998).

Isolation of *Ve1* homologues

The isolation of *Ve1* homologues from *N. glutinosa*, *S. tuberosum*, *S. torvum* and *H. lupulus* is described in Methods S1 and Tables S2–S4.

Binary over-expression constructs and transient expression *in planta*

For *NgVe1*, *StuVe1*, *StuVe2*, *StoVe1* and *StoVe2* constructs, CDS regions were amplified from *N. glutinosa*, *S. tuberosum* and *S. torvum* cDNA, respectively, whereas the CDS regions of *HLVe1-2A* and *HLVe1-2B* were amplified from the corresponding plasmids (Table S1). The CDS fragments were cloned into pDONR207 using Gateway® BP Clonase® II Enzyme Mix (Invitrogen, Carlsbad, CA, USA). All pDONR207 clones were sequenced, and fragments were subsequently transferred to pEarleyGate 100, pSol2095 (C-terminal GFP tag) (Zhang *et al.*, 2013a) or pFAST_R02 as described previously (Shimada *et al.*, 2010) using Gateway® LR Clonase® II Enzyme Mix (Invitrogen). Constructs for the constitutive expression of *Ave1*, *FoAve1*, *CbAve1* and *ChAve1* have been described previously (de Jonge *et al.*, 2012). *CoAve1* (Gan *et al.*, 2013) and *XacPNP* (Gottig *et al.*, 2008) were obtained by gene synthesis (Eurofins MWG Operon, Ebersberg, Germany), and subsequently recombined into the destination vector pSol2092 (Zhang *et al.*, 2013a) to generate expression constructs *pSol2092::CoAve1* and *pSol2092::XacPNP*. All constructs were transformed to *A. tumefaciens* strain GV3101 (pMP90) by electroporation.

Agrobacterium tumefaciens carrying expression constructs was infiltrated into tobacco plants as described previously (Zhang *et al.*, 2013a). *Agrobacterium tumefaciens* cultures containing constructs to express Ave1 and Ve1 homologues were mixed in a 1 : 1 ratio and infiltrated into the leaves of 5–6-week-old tobacco plants. At 5 days post-infiltration, photographs were taken, and necrosis was quantified using ImageJ to measure the area of necrosis as the percentage of the total infiltrated leaf area.

Protein extracts and immunoblotting

For the detection of GFP-tagged Ve1 homologues, *A. tumefaciens* carrying the corresponding expression constructs was infiltrated into mature tobacco leaves as described previously (Zhang *et al.*, 2013a). The co-immunopurifications and immunoblotting were performed as described previously (Zhang *et al.*, 2014).

Quantitative real-time PCR and reverse transcription-PCR (RT-PCR)

The target specificity of the constructs *TRV::GUS* and *TRV::NgVe1* was determined in TRV-infected *N. glutinosa* plants. Four weeks after TRV inoculation, whole tobacco plants were collected, frozen in liquid nitrogen and stored at −80°C for total RNA isolation.

For the expression of *Ve* homologues in the corresponding transgenic plants, 2-week-old Arabidopsis seedlings were harvested and ground into a powder in liquid nitrogen. Total RNA extraction, cDNA synthesis and RT-

PCR were performed as described previously (Zhang *et al.*, 2013b; Table S1). To analyse the expression of *NgVe1* in TRV-targeted *N. glutinosa* plants, quantitative real-time PCR was conducted using the primers NgVe1-F(qRT) and NgVe1-R(qRT) with tobacco *Actin* as an endogenous gene (Table S1), employing the qPCR Core Kit for SYBR Green I (Eurogentec Nederland BV, Maastricht, the Netherlands) as described previously (Fradin *et al.*, 2009).

VIGS

Constructs *pTRV2::PDS* and *pTRV2::GUS* were used as controls. To silence *NgVe1* in *N. glutinosa*, the construct *pTRV2::NgVe1* was generated. TRV vectors were agroinfiltrated as described previously (Liu *et al.*, 2002; Zhang *et al.*, 2013a). Briefly, cotyledons of 10–15-day-old *N. glutinosa* seedlings were infiltrated with 1 : 1 mixtures of *pTRV1* and *pTRV2* constructs. Photobleaching was observed at 4 weeks after agroinfiltration of *pTRV2::PDS*. For HR assays, 4 weeks after virus inoculations, mature leaves were agroinfiltrated to individually express *Ave1*, *VdNLP1* (Santhanam *et al.*, 2013) and *Avr9* (van Kan *et al.*, 1991; Van der Hoorn *et al.*, 2000). *VdNLP1* and *Avr9* were used as positive and negative controls, respectively. Five days after agroinfiltration, leaves were examined for the development of HR. For *Verticillium* disease assays, 3 weeks after TRV infection, the TRV-infected plants were inoculated with race 1 *V. dahliae* strain JR2 (Faino *et al.*, 2015), the corresponding *Ave1* deletion mutant (*V. dahliae* JR2 Δ*Ave1*; de Jonge *et al.*, 2012) and tap water as control. The inoculated plants were evaluated by the observation of disease symptoms at 14 dpi.

Disease assays

Verticillium dahliae was grown on potato dextrose agar at 22°C, and conidia were collected from 7–10-day-old plates and washed with tap water. *Verticillium* disease assays on *N. glutinosa* plants were performed as described previously (Zhang *et al.*, 2013a). Briefly, 5-week-old plants were uprooted, the roots were rinsed in water, dipped for 3 min in a suspension of 10^6 conidiospores/mL water and transferred to soil. *Verticillium* disease assays on *Arabidopsis*, as well as *Verticillium* biomass quantification in infected Arabidopsis plants, were performed as described previously (Ellendorff *et al.*, 2009).

Phylogenetic identification

To obtain the phylogenetic relationship of tomato Ve1 and its homologues, we identified similar sequences in 41 plant species acquired from Phytozome (v9.1) (Goodstein et al., 2012) and manually added Ve1 homologues of tobacco, potato, wild eggplant and hop. Sequence similarity was established using BLAST (version 322.28+), applying a conservative e-value cut-off of 1e-50. To prevent spurious hits, we removed sequences in which the matching area was less than 75% or the 'actual matching' was less than 50% of either Ve1 or the subject. The matching area is defined as the area from the start position of the first segment to the end position of the last segment, and the 'actual matching' area is defined as the sum of the covered area by each individual segment. Moreover, sequences that deviate in length (<80% or >120% of the length of Ve1) or contain protein domains other than leucine-rich repeats, as predicted by HMMER3 (version 3.0) (Finn et al., 2011) on a local PFAM database (version 27), were discarded. Subsequently, all protein sequences were aligned using MAFFT (version 7.047b) (Katoh et al., 2002) and the most consistent alignment (LINSI) was chosen using trimAl (version 1.2) (Capella-Gutiérrez et al., 2009), after which the heuristic method of trimAl was applied to trim the alignment. This cleaned alignment was used to construct an initial phylogenetic tree employing quick tree (version 1.1; 1000 bootstraps). The clade of interest (with tomato Ve1) and surrounding sequences were manually gathered and realigned. The final phylogenetic tree was inferred using RAxML (version 7.6.3) (Stamatakis, 2006), with the gamma model of rate heterogeneity and the Whelan and Goldman amino acid substitution matrix.

ACKNOWLEDGEMENTS

Y.S. acknowledges a fellowship from the China Scholarship Council. B.P.H.J.T. and M.F.S. were supported by a Vici and a Veni grant, respectively, from the Research Council for Earth and Life Sciences (ALW) of the Netherlands Organization for Scientific Research (NWO). B.J. and J.J. acknowledge financial support from the Slovenian Research Agency, Grant Number P4-0077, and the support of A.M. by a PhD grant (No. 1000-09-310205). Bert Essenstam is acknowledged for excellent plant care.

REFERENCES

Albert, I., Böhm, H., Albert, M., Feiler, C.E., Imkampe, J., Wallmeroth, N., Brancato, C., Raaymakers, T.M., Oome, S., Zhang, H., Krol, E., Grefen, C., Gust, A.A., Chai, J., Hedrich, R., Van den Ackerveken, G. and Nürnberger, T. (2015) An RLP23–SOBIR1–BAK1 complex mediates NLP-triggered immunity. *Nat. Plants*, **1**, 15140.

Antanaviciute, L., Šurbanovski, N., Harrison, N., McLeary, K., Simpson, D., Wilson, F., Sargent, D. and Harrison, R. (2015) Mapping QTL associated with *Verticillium dahliae* resistance in the cultivated strawberry (*Fragaria×ananassa*). *Hortic. Res.* **2**, 15009.

Bolek, Y., El-Zik, K.M., Pepper, A.E., Bell, A.A., Magill, C.W., Thaxton, P.M. and Reddy, O.U.K. (2005) Mapping of verticillium wilt resistance genes in cotton. *Plant Sci.* **168**, 1581–1590.

Boller, T. and Felix, G. (2009) A renaissance of elicitors: perception of microbe-associated molecular patterns and danger signals by pattern-recognition receptors. *Annu. Rev. Plant Biol.* **60**, 379–406.

Capella-Gutiérrez, S., Silla-Martínez, J.M. and Gabaldón T. (2009) trimAl: a tool for automated alignment trimming in large-scale phylogenetic analyses. *Bioinformatics*, **25**, 1972–1973.

Chai, Y., Zhao, L., Liao, Z., Sun, X., Zuo, K., Zhang, L. and Tang, K. (2003) Molecular cloning of a potential *Verticillium dahliae* resistance gene *SlVe1* with multi-site polyadenylation from *Solanum licopersicoides*. *DNA Seq.* **14**, 375–384.

Chen, T., Kan, J., Yang, Y., Ling, X., Chang, Y. and Zhang, B. (2016) A *Ve* homologous gene from *Gossypium barbadense*, *Gbvdr3*, enhances the defense response against *Verticillium dahliae*. *Plant Physiol. Biochem.* **98**, 101–111.

Christopoulou, M., Wo, S.R.-C., Kozik, A., McHale, L.K., Truco, M.-J., Wroblewski, T. and Michelmore, R. (2015) Genome-wide architecture of disease resistance genes in lettuce. *G3*, **5**, 2655–2669.

Clough, S.J. and Bent, A.F. (1998) Floral dip: a simplified method for *Agrobacterium*-mediated transformation of *Arabidopsis thaliana*. *Plant J.* **16**, 735–743.

Cook, D.E., Mesarich, C.H. and Thomma, B.P.H.J. (2015) Understanding plant immunity as a surveillance system to detect invasion. *Annu. Rev. Phytopathol.* **53**, 541–563.

Darby, P. (2001) 'Single gene traits in hop breeding'. *Proceedings of the Scientific Commission of the International Hop Growers Convention*, Canterbury, UK., (Seigner, E., ed.), 76–80.

Diwan, N., Fluhr, R., Eshed, Y., Zamir, D. and Tanksley, S. (1999) Mapping of *Ve* in tomato: a gene conferring resistance to the broad-spectrum pathogen, *Verticillium dahliae* race 1. *Theor. Appl. Genet.* **98**, 315–319.

Ellendorff, U., Fradin, E.F., de Jonge, R. and Thomma, B.P.H.J. (2009) RNA silencing is required for Arabidopsis defence against *Verticillium* wilt disease. *J. Exp. Bot.* **60**, 591–602.

Faino, L., Seidl, M.F., Datema, E., van den Berg, G.C., Janssen, A., Wittenberg, A.H. and Thomma, B.P.H.J. (2015) Single-molecule real-time sequencing combined with optical mapping yields completely finished fungal genome. *MBio*, **6**, e00936–15.

Fei, J., Chai, Y., Wang, J., Lin, J., Sun, X., Sun, C., Zuo, K. and Tang K. (2004) cDNA cloning and characterization of the *Ve* homologue gene *StVe* from *Solanum torvum* Swartz. *DNA Seq.* **15**, 88–95.

Finn, R.D., Clements, J. and Eddy, S.R. (2011) HMMER web server: interactive sequence similarity searching. *Nuc. Acids Res.* **39**, W29–W37.

Fradin, E.F. and Thomma, B.P.H.J. (2006) Physiology and molecular aspects of *Verticillium* wilt diseases caused by *V. dahliae* and *V. albo-atrum*. *Mol. Plant Pathol.* **7**, 71–86.

Fradin, E.F., Zhang, Z., Ayala, J.C.J., Castroverde, C.D., Nazar, R.N., Robb, J., Liu C.-M. and Thomma B.P.H.J. (2009) Genetic dissection of *Verticillium* wilt resistance mediated by tomato Ve1. *Plant Physiol.* **150**, 320–332.

Fradin, E.F., Abd-El-Haliem, A., Masini, L., van den Berg, G.C., Joosten, M.H. and Thomma, B.P.H.J. (2011) Interfamily transfer of tomato *Ve1* mediates *Verticillium* resistance in Arabidopsis. *Plant Physiol.* **156**, 2255–2265.

Fradin, E.F., Zhang, Z., Rovenich, H., Song, Y., Liebrand, T.W., Masini, L., van den Berg, G.C., Joosten, M.H. and Thomma, B.P.H.J. (2014) Functional analysis of the tomato immune receptor Ve1 through domain swaps with its non-functional homolog Ve2. *PLoS One*, **9**, e88208.

Fritz-Laylin, L.K., Krishnamurthy, N., Tör, M., Sjölander, K.V. and Jones, J.D. (2005) Phylogenomic analysis of the receptor-like proteins of rice and Arabidopsis. *Plant Physiol.* **138**, 611–623.

Gan, P., Ikeda, K., Irieda, H., Narusaka, M., O'Connell, R.J., Narusaka, Y., Takano, Y., Kubo, Y. and Shirasu, K. (2013) Comparative genomic and transcriptomic analyses reveal the hemibiotrophic stage shift of *Colletotrichum* fungi. *New Phytol.* **197**, 1236–1249.

Gijzen, M. and Nürnberger, T. (2006) Nep1-like proteins from plant pathogens: recruitment and diversification of the NPP1 domain across taxa. *Phytochemistry*, **67**, 1800–1807.

Goodstein, D.M., Shu, S., Howson, R., Neupane, R., Hayes, R.D., Fazo, J., Mitros, T., Dirks, W., Hellsten, U. and Putnam, N. (2012) Phytozome: a comparative platform for green plant genomics. *Nuc. Acids Res.* **40**, D1178–D1186.

Gottig, N., Garavaglia, B.S., Daurelio, L.D., Valentine, A., Gehring, C., Orellano, E.G. and Ottado, J. (2008) *Xanthomonas axonopodis* pv. *citri* uses a plant natriuretic peptide-like protein to modify host homeostasis. *Proc. Natl. Acad. Sci. USA*, **105**, 18 631–18 636.

Hayes, R.J., McHale, L.K., Vallad, G.E., Truco, M.J., Michelmore, R.W., Klosterman, S.J., Maruthachalam, K. and Subbarao, K.V. (2011) The inheritance of resistance to *Verticillium* wilt caused by race 1 isolates of *Verticillium dahliae* in the lettuce cultivar La Brillante. *Theor. Appl. Genet.* **123**, 509–517.

Inderbitzin, P., Davis, R.M., Bostock, R.M. and Subbarao, K.V. (2011) The ascomycete *Verticillium longisporum* is a hybrid and a plant pathogen with an expanded host range. *PLoS One*, **6**, e18260.

Jakse, J., Cerenak, A., Radisek, S., Satovic, Z., Luthar, Z. and Javornik, B. (2013) Identification of quantitative trait loci for resistance to Verticillium wilt and yield parameters in hop (*Humulus lupulus* L.). *Theor. Appl. Genet.* **126**, 1431–1443.

de Jonge, R., van Esse, H.P., Maruthachalam, K., Bolton, M.D., Santhanam, P., Saber, M.K., Zhang, Z., Usami, T., Lievens, B., Subbarao K.V. and Thomma, B.P.H.J. (2012) Tomato immune receptor Ve1 recognizes effector of multiple fungal pathogens uncovered by genome and RNA sequencing. *Proc. Natl. Acad. Sci. USA*, **109**, 5110–5115.

van Kan, J.A., Van den Ackerveken, G. and De Wit, P. (1991) Cloning and characterization of cDNA of avirulence gene *avr9* of the fungal pathogen *Cladosporium fulvum*, causal agent of tomato leaf mold. *Mol. Plant–Microbe Interact.* **4**, 52–59.

Katoh, K., Misawa, K., Kuma, K.i. and Miyata, T. (2002) MAFFT: a novel method for rapid multiple sequence alignment based on fast Fourier transform. *Nuc. Acids Res.* **30**, 3059–3066.

Kawchuk, L.M., Hachey, J., Lynch, D.R., Kulcsar, F., van Rooijen, G., Waterer, D.R., Robertson, A., Kokko, E., Byers, R., Howard, R.J., Fischer, R. and Prufer, D. (2001) Tomato *Ve* disease resistance genes encode cell surface-like receptors. *Proc. Natl. Acad. Sci. USA*, **98**, 6511–6515.

Liu, S., Zhu, Y., Xie, C., Jue, D., Hong, Y., Chen, M., Hubdar, A.K. and Yang, Q. (2012) Transgenic potato plants expressing *StoVe1* exhibit enhanced resistance to *Verticillium dahliae*. *Plant Mol. Biol. Rep.* **30**, 1032–1039.

Liu, Y., Schiff, M. and Dinesh-Kumar, S. (2002) Virus-induced gene silencing in tomato. *Plant J.* **31**, 777–786.

Macho, A.P. and Zipfel, C. (2014) Plant PRRs and the activation of innate immune signaling. *Mol. Cell*, **54**, 263–272.

Majer, A., Javornik, B., Cerenak, A. and Jakse, J. (2014) Development of novel EST-derived resistance gene markers in hop (*Humulus lupulus* L.). *Mol. Breed.* **33**, 61–74.

Santhanam, P., van Esse, H.P., Albert, I., Faino, L., Nürnberger, T. and Thomma, B.P.H.J. (2013) Evidence for functional diversification within a fungal NEP1-like protein family. *Mol. Plant–Microbe Interact.* **26**, 278–286.

Senthil-Kumar, M., Hema, R., Anand, A., Kang, L., Udayakumar, M. and Mysore, K.S. (2007) A systematic study to determine the extent of gene silencing in *Nicotiana benthamiana* and other Solanaceae species when heterologous gene sequences are used for virus-induced gene silencing. *New Phytol.* **176**, 782–791.

Shibuya, N. and Desaki, Y. (2015) Immunity: one receptor, many pathogens. *Nat. Plants*, **1**, 15149.

Shimada, T.L., Shimada, T. and Hara-Nishimura, I. (2010) A rapid and non-destructive screenable marker, FAST, for identifying transformed seeds of *Arabidopsis thaliana*. *Plant J.* **61**, 519–528.

Simko, I., Costanzo, S., Haynes, K., Christ, B. and Jones, R. (2004a) Linkage disequilibrium mapping of a *Verticillium dahliae* resistance quantitative trait locus in tetraploid potato (*Solanum tuberosum*) through a candidate gene approach. *Theor. Appl. Genet.* **108**, 217–224.

Simko, I., Haynes, K., Ewing, E., Costanzo, S., Christ, B. and Jones, R. (2004b) Mapping genes for resistance to *Verticillium albo-atrum* in tetraploid and diploid potato populations using haplotype association tests and genetic linkage analysis. *Mol. Genet. Genomics*, **271**, 522–531.

Stamatakis, A. (2006) RAxML-VI-HPC: maximum likelihood-based phylogenetic analyses with thousands of taxa and mixed models. *Bioinformatics*, **22**, 2688–2690.

Tang, J., Lin, J., Yang, Y., Chen, T., Ling, X., Zhang, B. and Chang, Y. (2016) Ectopic expression of a *Ve* homolog *VvVe* gene from *Vitis vinifera* enhances defense response to *Verticillium dahliae* infection in tobacco. *Gene*, **576**, 492–498.

Terauchi, R. and Kahl, G. (2000) Rapid isolation of promoter sequences by TAIL-PCR: the 5′-flanking regions of *Pal* and *Pgi* genes from yams (Dioscorea). *Mol. Gen. Genet.* **263**, 554–560.

Thomma, B.P.H.J., Nürnberger, T. and Joosten, M.H. (2011) Of PAMPs and effectors: the blurred PTI–ETI dichotomy. *Plant Cell*, **23**, 4–15.

Van der Hoorn, R.A., Laurent, F., Roth, R. and De Wit, P.J. (2000) Agroinfiltration is a versatile tool that facilitates comparative analyses of Avr 9/Cf-9-induced and Avr 4/Cf-4-induced necrosis. *Mol. Plant–Microbe Interact.* **13**, 439–446.

Vining, K. and Davis, T. (2009) Isolation of a *Ve* homolog, *mVe1*, and its relationship to verticillium wilt resistance in *Mentha longifolia* (L.) Huds. *Mol. Genet. Genomics*, **282**, 173–184.

Wang, G., Ellendorff, U., Kemp, B., Mansfield, J.W., Forsyth, A., Mitchell, K., Bastas, K., Liu, C.-M., Woods-Tör, A., Zipfel, C., De Wit, P.J., Jones, J.D.G., Tör, M. and Thomma, B.P.H.J. (2008) A genome-wide functional investigation into the roles of receptor-like proteins in Arabidopsis. *Plant Physiol.* **147**, 503–517.

Wang, G., Fiers, M., Ellendorff, U., Wang, Z., de Wit, P.J., Angenent, G.C. and Thomma, B.P.H.J. (2010) The diverse roles of extracellular leucine-rich repeat-containing receptor-like proteins in plants. *Crit. Rev. Plant Sci.* **29**, 285–299.

Wang, H.M., Lin, Z.X., Zhang, X.L., Chen, W., Guo, X.P., Nie, Y.C. and Li, Y.H. (2008) Mapping and quantitative trait loci analysis of *Verticillium* wilt resistance genes in cotton. *J. Integr. Plant Biol.* **50**, 174–182.

Xu, X., Pan, S., Cheng, S., Zhang, B., Mu, D., Ni, P., Zhang, G., Yang, S., Li, R., Wang, J., Orjeda, G., Guzman, F., Torres, M., Lozano, R., Ponce, O., Martinez, D., De la Cruz, G., Chakrabarti, S.K., Patil, V.U., Skryabin, K.G., Kuznetsov, B.B., Ravin, N.V., Kolganova, T.V., Beletsky, A.V., Mardanov, A.V., Di Genova, A., Bolser, D.M., Martin, D.M., Li, G., Yang, Y., Kuang, H., Hu, Q., Xiong, X., Bishop, G.J., Sagredo, B., Mejía, N., Zagorski, W., Gromadka, R., Gawor, J., Szczesny, P., Huang, S., Zhang, Z., Liang, C., He, J., Li, Y., He, Y., Xu, J., Zhang, Y., Xie, B., Du, Y., Qu, D., Bonierbale, M., Ghislain, M., Herrera Mdel, R., Giuliano, G., Pietrella, M., Perrotta, G., Facella, P., O'Brien, K., Feingold, S.E., Barreiro, L.E., Massa, G.A., Diambra,

L., Whitty, B.R., Vaillancourt, B., Lin, H., Massa, A.N., Geoffroy, M., Lundback, S., DellaPenna, D., Buell, C.R., Sharma, S.K., Marshall, D.F., Waugh, R., Bryan, G.J., Destefanis, M., Nagy, I., Milbourne, D., Thomson, S.J., Fiers, M., Jacobs, J.M., Nielsen, K.L., Sønderkær, M., Iovene, M., Torres, G.A., Jiang, J., Veilleux, R.E., Bachem, C.W., de Boer, J., Borm, T., Kloosterman, B., van Eck, H., Datema, E., Hekkert, B.T., Goverse, A., van Ham, R.C. and Visser, R.G. (2011) Genome sequence and analysis of the tuber crop potato. *Nature*, **475**, 189–197.

Yang, C., Guo, W., Li, G., Gao, F., Lin, S. and Zhang, T. (2008) QTLs mapping for *Verticillium* wilt resistance at seedling and maturity stages in *Gossypium barbadense* L. *Plant Sci.* **174**, 290–298.

Yang, Y., Ling, X., Chen, T., Cai, L., Liu, T., Wang, J., Fan, X., Ren, Y., Yuan, H., Zhu, W., Zhang, B. and Ma, D.-P. (2014) A cotton *Gbvdr5* gene encoding a leucine-rich-repeat receptor-like protein confers resistance to *Verticillium dahliae* in transgenic *Arabidopsis* and upland cotton. *Plant Mol. Biol. Rep.* **33**, 1–15.

Zhang, B., Yang, Y., Chen, T., Yu, W., Liu, T., Li, H., Fan, X., Ren, Y., Shen, D., Liu, L., Liu, L., Dou, D. and Chang, Y. (2012) Island cotton *Gbve1* gene encoding a receptor-like protein confers resistance to both defoliating and non-defoliating isolates of *Verticillium dahliae*. *PLoS One*, **7**, e51091.

Zhang, Y., Wang, X., Yang, S., Chi, J., Zhang, G. and Ma, Z. (2011) Cloning and characterization of a *Verticillium* wilt resistance gene from *Gossypium barbadense* and functional analysis in *Arabidopsis thaliana*. *Plant Cell Rep.* **30**, 2085–2096.

Zhang, Z. and Thomma, B.P.H.J. (2013) Structure–function aspects of extracellular leucine-rich repeat-containing cell surface receptors in plants. *J. Integr. Plant. Biol.* **55**, 1212–1223.

Zhang, Z., Fradin, E., de Jonge, R., van Esse, H.P., Smit, P., Liu, C.M. and Thomma, B.P.H.J. (2013a) Optimized agroinfiltration and virus-induced gene silencing to study Ve1-mediated *Verticillium* resistance in tobacco. *Mol. Plant–Microbe Interact.* **26**, 182–190.

Zhang, Z., Esse, H.P., Damme, M., Fradin, E.F., Liu, C.M. and Thomma, B.P.H.J. (2013b) Ve1-mediated resistance against *Verticillium* does not involve a hypersensitive response in Arabidopsis. *Mol. Plant Pathol.* **14**, 719–727.

Zhang, Z., Song, Y., Liu, C.M. and Thomma, B.P.H.J. (2014) Mutational analysis of the Ve1 immune receptor that mediates *Verticillium* resistance in tomato. *PLoS One*, **9**, e99511.

SUPPORTING INFORMATION

Additional Supporting Information may be found in the online version of this article at the publisher's website:

Fig. S1. Percentage of amino acid identity shared between nine Ve1 homologues. The highest percentage of homology between two Ve1 homologues is indicated in red. Dashes (-) represent identical sequences.

Fig. S2. Stability of green fluorescent protein (GFP)-fused NgVe1 protein *in planta*. Total protein extracts of transiently transformed leaf tissue were subjected to immunopurification (IP) using GFP-affinity beads. Immunopurified proteins were subjected to sodium dodecylsulfate-polyacrylamide gel electrophoresis (SDS/PAGE) and immunoblotted (IB) using α-GFP antibody. Coomassie blue staining (CBS) of the blot containing total protein extracts showed equal loading in each lane based on the 50-kDa RuBisCo (ribulose-1,5-bisphosphate carboxylase/oxygenase) band. GFP-tagged Ve1 protein was used as a control.

Fig. S3. *Tobacco rattle virus* (TRV)-mediated gene silencing in *Nicotiana glutinosa*. (A) Virus-induced gene silencing of the *phytoene desaturase* (*PDS*) gene results in patchy photobleaching in leaves of *N. glutinosa*. Photographs were taken at 4 weeks after *TRV::PDS* infiltration, and show representative infected plants of at least three independent assays. (B) *TRV::NgVe1*-inoculated plants show resistance to *Verticillium dahliae* strain JR2, but not *V. dahliae* JR2 Δ*Ave1*. *Nicotiana glutinosa* plants were inoculated with a recombinant TRV targeting the β-*glucuronidase* (*GUS*) gene as a control (*TRV::GUS*) or recombinant TRV targeting the *NgVe1* gene (*TRV::NgVe1*). At 3 weeks after TRV infiltration, TRV-inoculated plants were inoculated with either *V. dahliae* strain JR2 or *V. dahliae* JR2 Δ*Ave1* mutant. Photographs were taken 2 weeks after *V. dahliae* inoculation, and show representative inoculated plants of at least three independent assays. (C) Silencing efficiency was determined using quantitative real-time polymerase chain reaction at 28 days post-infiltration in *TRV::NgVe1*- and *TRV::GUS*-inoculated *N. glutinosa* plants. Bars represent levels of *NgVe1* transcripts relative to the transcript levels of *N. glutinosa actin* (for normalization) with standard deviation of a sample of three pooled plants. *NgVe1* expression in *TRV::GUS*-infected plants is set to unity.

Fig. S4. Expression of *NgVe1*, *HLVe1-2A*, *HLVe1-2B*, *StuVe1*, *StuVe2*, *StoVe1* and *StoVe2* in transgenic plants was detected by reverse transcription-polymerase chain reaction (RT-PCR). As an endogenous control, a fragment of the *AtRuBisCo* gene (RuBisCo, ribulose-1,5-bisphosphate carboxylase/oxygenase) was amplified from cDNA. For each construct, three independent transgenic lines are shown (1, 2 and 3). Water was used as a control.

Fig. S5. Southern blotting of seven hop cultivars with the tomato *Ve1* gene as a probe reveals the presence of *Ve*-like sequences in the hop genome. Seven hop cultivars are indicated: 1, 'Wye target'; 2, 'Fuggle'; 3, 'Wye Challenger'; 4, 'Savinjski Golding'; 5, 'Aurora'; 6, 'Celeia'; 7, 'Yeoman'. Hop genomic DNA was digested with the restriction enzymes *Eco*RI, *Eco*RV and *Hind*III, separated on 0.8% agarose gel and blotted on nylon membranes with the ^{32}P-labelled tomato *Ve1* gene sequence as a probe.

Fig. S6. Primary structure and protein sequence alignment of functional Ve1 proteins from tomato, tobacco, potato, wild eggplant and hop. The N-terminal amino acids in the dashed frame denote the predicted signal peptides (SPs) of the functional Ve1 homologues. eLRR, extracellular leucine-rich repeat (C1 domain and C3 domain); IS, non-LRR island domain (C2 domain); AC, acidic domain; TM, transmembrane domain; CT, cytoplasmic domain. The locations of the predicted solvent-exposed β-sheet (xxLxLxx) on the concave surface of the receptor are indicated above the eLRR domains. Identical amino acid residues are highlighted in red, whereas conserved amino acid residues are highlighted in blue. Three consecutive eLRR regions required for the functionality of Ve1 are indicated by bold colour, whereas other regions that could not be implicated in Ve1 functionality are indicated in light colour. Ve1 homologue sequences can be found in the GenBank database using

the following GenBank accessions: ACR33105 (Ve1), ALK26499 (NgVe1), ALK26501 (StuVe1), ALK26500 (StoVe1), AIE39594 (HLVe1-2A).

Fig. S7. Percentage of amino acid identity shared between the C1 domain, C2 domain, C3 domain and C-terminal extracellular leucine-rich repeat (eLRR)-flanking domain of the functional and non-functional Ve1 homologues from tomato, tobacco, potato, wild eggplant and hop.

Fig. S8. An unrooted phylogenetic tree based on protein sequences of Ve1 homologues from the tomato clade and the relevant sister clades. The tomato Ve1 clade is indicated by the highlighted background. Official gene identifiers and species names are indicated. Bootstrap values are shown in the tree. The scale represents branch lengths expressed as the relative number of amino acid substitutions.

Table S1. Primers used for amplification, sequencing and expression of *Ve1* homologues.

Table S2. Degenerative primers used for thermal asymmetric interlaced-polymerase chain reaction (TAIL-PCR) amplification of the flanking regions of putative hop *Ve1* homologues.

Table S3. Primers used for the thermal asymmetric interlaced-polymerase chain reaction (TAIL-PCR)-based isolation of hop *Ve1* sequences.

Table S4. Amplification conditions used for thermal asymmetric interlaced-polymerase chain reaction (TAIL-PCR).

Methods S1. Isolation of *Ve1* homologues.